

## Nuclear-magnetic-resonance study of the electronic structure of the Ti-H system

Charles Korn\*

*Department of Physics, Ben Gurion University of the Negev, Beer Sheva, Israel*

(Received 25 March 1975; revised manuscript received 19 August 1976)

The proton spin-lattice relaxation time  $T_1$  of hydrogen in titanium hydride was measured as a function of temperature and hydrogen concentration in the temperature range where the overriding relaxation mechanism is the interaction with the conduction electrons. The hydrogen-concentration dependence and the temperature dependence of  $(T_1 T)^{-1/2}$  is presented. A break in the temperature dependence curve of  $(T_1 T)^{-1/2}$  was found for hydrogen concentrations having atomic ratios greater than 1.8. This is associated with a tetragonal deformation which is known to occur for the hydride. A phenomenological model of the electronic structure based on a semirigid band is proposed to explain the data. The concentration and temperature dependence of the susceptibility, hyperfine interactions, and transport properties are discussed in terms of the proposed model as well as the cause of the tetragonal deformation and the low-hydrogen-concentration limit of the hydride.

### I. INTRODUCTION

The problem of the electronic structure of transition-metal hydrides has often been approached in terms of the rigid-band model of metals and alloys. The controversy over the effect of the addition of hydrogen to metals has been widely discussed with many varying and conflicting ideas proposed.<sup>1</sup> Thus for example one of the early<sup>2</sup> (although disputed<sup>3</sup>) attempts in explaining the decrease of the susceptibility of palladium upon the absorption of hydrogen, was based on the filling up of the  $d$  band with electrons which the hydrogen donates. This interpretation was given theoretical support by Isenberg<sup>4</sup> who calculated that charge screening should prevent the dissolved hydrogen from retaining a bound state in any metal, thus causing the hydrogen to contribute its electron to the conduction band. The work of Zamir<sup>5</sup> comparing the Knight shifts and spin-lattice relaxation times in V-Cr and Nb-Mo alloys with V-H and Nb-H, and the subsequent measurements of Rohy and Cotts<sup>6,7</sup> on the V-Cr-H system tend to support a rigid-band model where each hydrogen atom contributes one electron to the conduction band. Schreiber, Cotts, and Merriam<sup>8-10</sup> also use this model to interpret their NMR measurements on the La-H system. Bos, Gutowsky, and Green,<sup>11,12</sup> on the other hand, explain the La-H system using a rigid-band model in which the hydrogen serves to deplete the band. Switendick<sup>13</sup> challenges the rigid-band model for the metal-hydrogen system from band-structure calculations and Nagel and Goretzki<sup>14</sup> interpret their susceptibility measurement results on Ti-V-H in support of Switendick's contentions.

In this study, nuclear-magnetic-resonance measurements were carried out on the Ti-H system in order to contribute to an understanding of the electronic structure and physical properties of this

transition-metal hydride. Hyperfine interactions with the conduction electrons cause nuclei in a magnetic field to relax,<sup>15</sup> making the NMR method a useful probe in such a study. The nuclear spin-lattice relaxation time  $T_1$  of hydrogen in titanium hydride was measured as a function of temperature and hydrogen concentration in a temperature region where the primary relaxation mechanism is due to the conduction electrons. A phenomenological model of the electronic structure of the Ti-H system and the role of hydrogen will be introduced in order to interpret the data and attempts will be made to correlate other measurements as well as some physical properties of the hydride with the proposed model.

The proton spin-lattice relaxation times in Ti-H were also obtained by Torrey,<sup>16</sup> Korn and Zamir,<sup>17</sup> Schmolz and Noack,<sup>18</sup> and Khodosov and Shepilov.<sup>19</sup> The studies of Torrey, Korn *et al.*, and Schmolz *et al.* were mainly concerned with diffusion and so were conducted mostly at elevated temperatures, although a strong conduction-electron contribution was obtained near room temperature. The low-temperature relaxation times reported by Khodosov *et al.* did not agree with our results, being for certain points as much as  $\frac{1}{5}$  the values quoted here.

Titanium has an hcp structure ( $\alpha$  phase), and below 125 °C practically no hydrogen dissolves in this phase. A hydride is formed instead, having a composition range  $1.5 \leq x \leq 2.0$ , where  $x$  is the ratio of hydrogen to titanium atoms, the hydride being designated by  $\text{TiH}_x$ . The hydride has an fcc structure<sup>20</sup> with the hydrogen randomly occupying the tetrahedral sites.<sup>21,22</sup> A tetragonal deformation occurs below about 35 °C for high hydrogen concentrations.<sup>20,23</sup> The phase diagram can be found in Ref. 17.

Following the Introduction, Sec. II describes the experimental procedure while the experimental

results are reported in Sec. III. The phenomenological theory of the electronic structure introduced in order to explain these results is based on a semirigid-band model. This model must be judged not only on its ability to interpret our present measurements, but also on how well it correlates various other properties of the hydride. Thus it will be necessary to present some of the known characteristics of the hydride. Section IV A is devoted to some of the background material; the model is introduced in Sec. IV B, while Secs. IV C and IV D discuss the hyperfine interactions and thermal effects in terms of the proposed model. Some general remarks on bonding in the hydride are made in Sec. IV E. Section V reviews and highlights the main points.

## II. EXPERIMENTAL PROCEDURE

Sample preparation was described previously.<sup>17</sup> The spin-lattice relaxation time  $T_1$  of hydrogen was measured at 24 MHz using a Bruker B-KR 321s pulsed spectrometer.  $T_1$  was obtained by flipping the spins with an initial  $180^\circ$  pulse and measuring the signal amplitude following a second  $90^\circ$  sampling pulse as a function of time between the two pulses. The growth of nuclear magnetization was observed over an amplitude of approximately  $1\frac{1}{2}$  decades and was found to increase exponentially giving a well defined  $T_1$ .  $H_1$  was approximately 50 G which is about four times the dipolar linewidth. Signals were recorded using a box car integrator which sampled the beginning of the free-induction decay for a small fraction of the spin-spin relaxation time  $T_2$ . The time between pulse pairs was taken to be about  $10T_1$ . The temperature ranged from 100 to 350 °K; the low value being limited by our present instrumentation and the high value chosen to overlap the region where a cubic-tetragonal transition takes place but does not yet contain a significant diffusional relaxation contribution.

For reasons to be described later, the Knight shift of hydrogen in titanium wire was obtained for various orientations of the wire with respect to the external magnetic field. The sample composition was  $\text{TiH}_{1.80}$  and it was prepared by hydriding Materials Research 0.005-in.-diam wire drawn from zone-refined titanium. Small lengths of wire were placed in Pyrex capillaries which were then mechanically oriented in one direction. The ends of the capillaries were closed off with very thin sheets of parafilm which also served as a reference. (The proton resonance of the parafilm was measured separately with respect to water and no shift was detected.) The shift was obtained from steady-state absorption traces using a Varian wide line transmitting and

receiving system and a Princeton Applied Research phase detector. The Varian crossed-coil probe was hydrogen free and measurements were conducted at 16 MHz.

## III. EXPERIMENTAL RESULTS

The spin-lattice relaxation time  $T_1$  was obtained as a function of temperature for hydrogen concentrations  $x=1.55, 1.70, 1.81, 1.90,$  and  $1.99$ , where  $x$  is the ratio of the number of hydrogen to titanium atoms. The results are shown in Fig. 1.  $T_1$  can be separated into its hydrogen diffusion  $T_{1d}$  and conduction electron  $T_{1e}$  contributions, using the relation  $(T_1)^{-1} = (T_{1d})^{-1} + (T_{1e})^{-1}$ .  $T_{1d}$  is known from a diffusion study conducted at higher temperatures.<sup>17</sup> This contribution is quite negligible compared to  $T_{1e}$  and has a slight influence only above 310 °K for low hydrogen concentration samples where diffusion is faster. The resulting  $T_{1e}$  values are also shown in Fig. 1.

$T_1$  was also measured as a function of hydrogen concentration  $x$ . Here the temperature controller was kept at the same setting and different samples were inserted into the probe. It is expected that with this method, errors connected with the

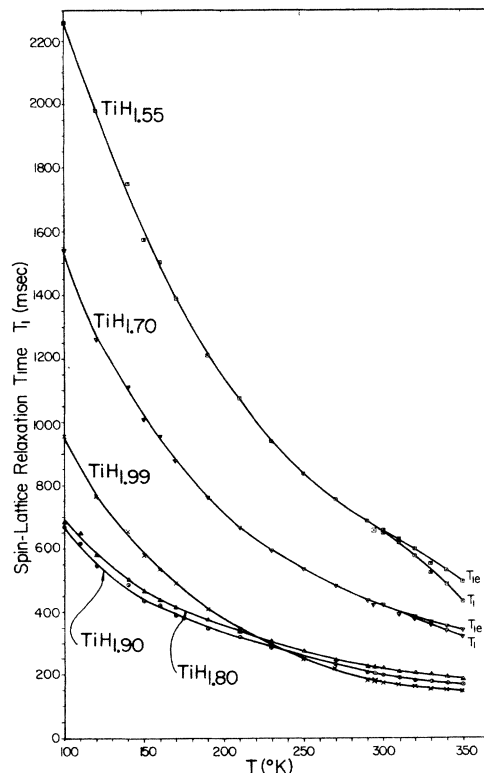


FIG. 1. Temperature dependence of  $T_1$  and  $T_{1e}$  (essentially equal to  $T_1$  over most of the range) for various hydrogen concentrations.

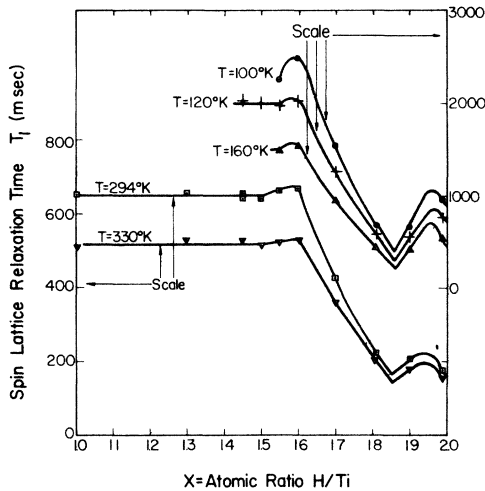


FIG. 2. Hydrogen concentration dependence of  $T_1$  at various temperatures.

reproducibility of the temperature are minimized. The results are shown in Fig. 2. The variation of  $T_1$  with hydrogen concentration is shown: (a) for low temperatures (100, 120, 160 °K); (b) at a temperature (330 °K) just above the (to be discussed) tetragonal deformation; and (c) at 294 °K which is just below the transition temperature. A curve is sketched through the experimental points in such a manner as to agree with the variation expected from susceptibility measurements<sup>24</sup> and the electronic band model to be discussed. It will be noted that below  $x=1.5$  the relaxation time is independent of the total concentration, which is as expected since the hydrogen is always in the  $\gamma$  phase having a local concentration of  $x=1.5$ .

Above  $x=1.5$ ,  $T_1$  increases slightly and then drops quickly in going from  $x=1.6$  to  $x=1.8$ . (The interpretation of Ref. 17 attributing the slight initial rise to the effect of diffusion is incorrect since this contribution is negligible at low temperatures.)

In our subsequent discussion we will find it worthwhile to compare our  $T_{1e}$  results with the proton Knight shift. A detailed study of this shift in Ti-H was carried out by Stalinski, Coogan, and Gutowsky.<sup>22</sup> Schreiber and Graham<sup>25</sup> questioned the validity of these results on the basis of effects arising from macroscopic demagnetization fields which depend on the geometric shape of the sample. The hydrogen Knight shifts in Ti-H measured by Frisch and Forman<sup>26</sup> do not agree with those of Stalinski *et al.* and they cite Schreiber and Graham's suggestion to explain the discrepancy. In order to check whether the effect is large enough to be significant in our case, measurements were carried out for the limiting case

of titanium hydride wires. If there were no true Knight shift,  $\Delta H/H$  should be positive when the wires are oriented along the external field and negative when they are perpendicular to the external field. We measured the shift along and perpendicular to the external field and no orientation dependence was detected. The shifts were small fractions of the linewidth. This together with the small sample size resulted in a fairly large error (of the order of  $\frac{1}{4}$  of the measured shift). The shifts expected from the macroscopic susceptibility can be estimated from Trzebiatowsky *et al.* susceptibility measurements<sup>24</sup> to be about  $-0.003\%$  for the wires perpendicular to the field and  $+0.007\%$  for the wires along the field. We obtained  $K = -0.012 \pm 0.003\%$  where the error is the root mean square of ten measurements. This is equal to the Knight shift obtained by Stalinski *et al.* for this concentration ( $x=1.8$ ). We thus conclude that the negative Knight shift is real for the case of titanium hydride and that the macroscopic susceptibility effects are within the range of experimental error.

#### IV. DISCUSSION

##### A. General background

Let us first break up the magnetic interactions for a transition metal in the usual way.<sup>27</sup> If the subscript  $s$  refers to the spin interaction of the  $s$  conduction-band electrons,  $d$  refers to the  $d$ -band electron-spin contribution, and  $o$  to the orbital paramagnetic contribution of the  $d$  electrons, then the total magnetic susceptibility  $\chi$  can be written

$$\chi = \chi_s + \chi_d + \chi_o \approx 2A \mu_B^2 N_s(E_F) + 2A \mu_B^2 N_d(E_F) + \chi_o, \quad (1)$$

where the relatively small (for transition metals) diamagnetic contribution is neglected.  $N(E)$  is the density of states for one direction of the spin,  $E_F$  is the energy at the Fermi level,  $A$  is Avogadro's number, and  $\mu_B$  is the Bohr magneton. Thus the spin contributions are proportional to the density of states (in contrast to  $\chi_o$ ) and since for transition metals  $N_d(E_F) \gg N_s(E_F)$ , the  $d$  electrons are the dominating factor in the spin susceptibility.

Similarly for the Knight shift<sup>27</sup>  $K$

$$\begin{aligned} K &= K_s + K_d + K_o = (1/A \mu_B) (H_{\text{hf}}^{(s)} \chi_s + H_{\text{hf}}^{(d)} \chi_d + H_{\text{hf}}^{(o)} \chi_o) \\ &= 2 \mu_B [ H_{\text{hf}}^{(s)} N_s(E_F) + H_{\text{hf}}^{(d)} N_d(E_F) ] \\ &\quad + (1/A \mu_B) H_{\text{hf}}^{(o)} \chi_o, \end{aligned} \quad (2)$$

where  $H_{\text{hf}}$  are the respective hyperfine fields at the nucleus. The  $s$  term is due to the contact interaction which gives a positive contribution while the  $d$  term is due to core polarization and contributes a negative shift. The orbital contribu-

tion to the shift is generally positive for the metal nucleus. The prime on  $H_{\text{hf}}^{(0) \prime}$  implies an average over all contributing states of the  $d$  band in calculating the orbital hyperfine field  $H_{\text{hf}}^{(0) \prime} = 2\mu_B \langle r^{-3} \rangle_D$ . Whereas the contact and core polarization terms in the Knight shift depend only on electrons at the Fermi level, this is not so for the orbital contribution.

The corresponding spin-lattice relaxation contributions give<sup>27</sup>

$$1/T_{1e} = 4\pi\gamma_n^2 \hbar k_B T \{ [H_{\text{hf}}^{(s)} N_s(E_F)]^2 + [H_{\text{hf}}^{(d)} N_d(E_F)]^2 q + [H_{\text{hf}}^{(o)} N_d(E_F)]^2 p \}, \quad (3)$$

where  $T$  is the temperature,  $k_B$  is the Boltzmann constant,  $p$  and  $q$  are reduction factors, and  $H_{\text{hf}}^{(o)} = 2\mu_B \langle r^{-3} \rangle_d$ , where now the subscript  $d$  refers to an average over electron states at the Fermi level only. Thus the orbital contribution to the relaxation rate depends only on the electronic states at the Fermi level, in contrast to the behavior of the orbital Knight shift. Usually the approximation  $\langle r^{-3} \rangle_d \approx \langle r^{-3} \rangle_D$ ,  $H_{\text{hf}}^{(o)} \approx H_{\text{hf}}^{(0) \prime}$  is made.<sup>28</sup>

If now in our case we assume that one of the relaxation terms dominates, then  $(T_{1e} T)^{-1/2}$  should be approximately proportional to the density of states at the Fermi level  $N(E_F)$ . By plotting the former parameter as a function of hydrogen concentration, the behavior of the latter may be inferred. Figure 3(a) presents this relationship. The curves through the points have been drawn in a manner so as to facilitate later discussion and emphasize the similarities to the magnetic susceptibility behavior shown in Fig. 3(b) (data of Trzebiatowsky and Stalinski<sup>24</sup>). Figure 3(c) shows the proton Knight shift as a function of hydrogen concentration obtained by Stalinski, Coogan, and Gutowsky,<sup>13</sup> while Fig. 3(d) gives the variation of the crystallographic structure with hydrogen concentration obtained by Azarkh *et al.*<sup>23</sup>

The concentration dependence of the four parameters shown in Fig. 3 have been placed one above the other to illustrate their connection. Going from a low to a high hydrogen concentration,  $(T_{1e} T)^{-1/2}$  deviates from a constant value at  $x=1.5$ , where crystallographically the pure hydride phase begins.  $(T_{1e} T)^{-1/2}$  is expected to remain constant below  $x=1.5$  since the hydrogen in an environment having the same hydrogen concentration of  $x=1.5$ . At  $x=1.5$ ,  $(T_{1e} T)^{-1/2}$  first dips slightly and then increases rapidly up to  $x=1.8$ . At  $x=1.8$  there is an abrupt change in curvature. Near this concentration a low-temperature tetragonal deformation begins. (The exact concentration where this transformation takes place is somewhat in dispute—see, for example, Irving and Beevers<sup>29</sup>—and the question

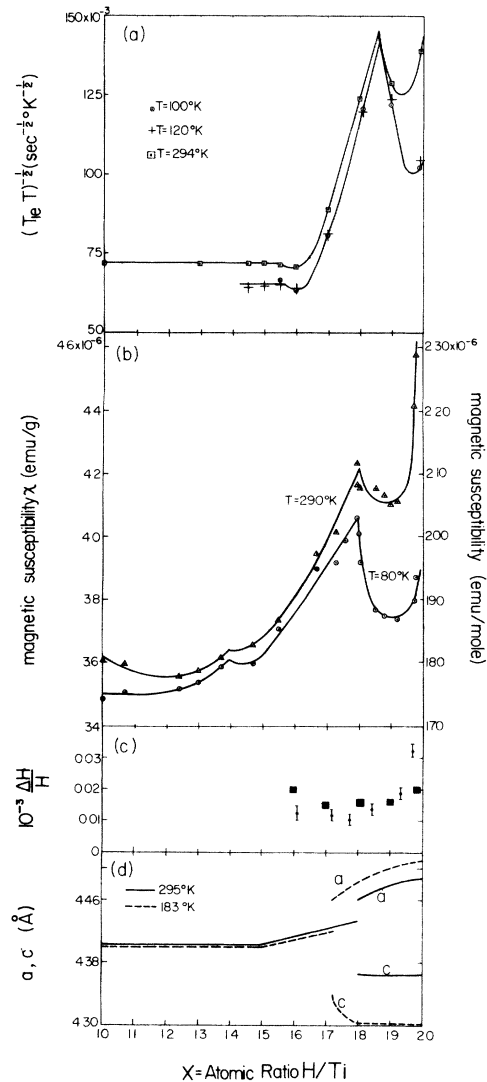


FIG. 3. Concentration dependence of various properties of Ti-H. (a)  $(T_{1e} T)^{-1/2}$ —data of this study. (b) Magnetic susceptibility  $\chi$ —data of Trzebiatowsky *et al.* (Ref. 24). (c) Knight shift  $K$ —data of Stalinski *et al.* (Ref. 22). Darkened squares are derived from our  $T_1$  data as described in text. (d) Lattice parameters  $a, c$ —data of Azarkh *et al.* (Ref. 23).

will be discussed in more detail in Sec. IV D). This is followed by a trough in  $(T_{1e} T)^{-1/2}$ . It is necessary to dispel the following idea: that actually  $(T_{1e} T)^{-1/2}$  is low in the low-concentration cubic phase, high in the tetragonal phase, and the rise we see between  $x=1.6$  and  $x=1.8$  is simply due to a two-phase region with more and more tetragonal phase being represented as the concentration is increased. If this were so, we would expect to see two simultaneous relaxation rates giving a non-exponential spin-lattice relaxation. Such a large

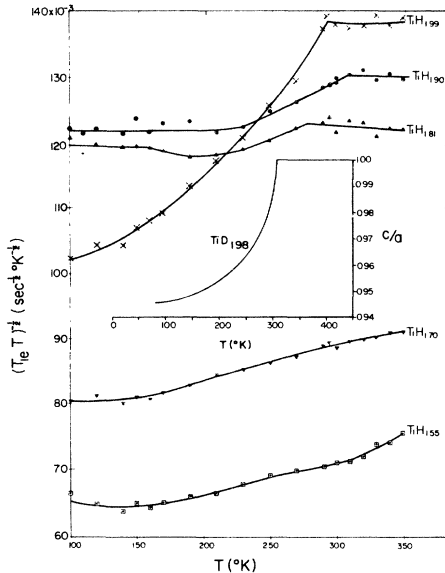


FIG. 4. Temperature dependence of  $(T_{1e}T)^{-1/2}$  for various hydrogen concentrations. The break in curvature for the higher hydrogen concentrations is associated with the tetragonal-cubic phase transition. Compare curve for  $x=1.99$  with tetragonality shown in insert [insert data—Yakel (Ref. 20)].

disparity in  $T_1$  would easily have been detected. Second, the  $T_1$ -vs- $x$  curve above the transition temperature shows a behavior similar to that below this temperature (Fig. 2).

While the shape of the susceptibility curves are similar to that of  $(T_{1e}T)^{-1/2}$ , the scale shows that the percentage change of the former is much smaller. Also of significance is that the Knight shift does not follow the behavior of  $(T_{1e}T)^{-1/2}$  and  $\chi$ . It has no cusplike shape and is practically constant between  $x=1.6$  and  $x=1.8$ , the region where  $(T_{1e}T)^{-1/2}$  and  $\chi$  show a significant rise. Our model for the electronic structure will attempt to correlate these phenomena.

We now discuss the temperature dependence of the interactions. The temperature dependence of  $T_1$  shown in Fig. 1 does not in itself indicate anything of significance. If however, the data is replotted to give  $(T_{1e}T)^{-1/2}$  as a function of  $T$ , we obtain the results shown in Fig. 4. At this point we only emphasize the sharp rise for  $\text{TiH}_{1.99}$  and the more modest rises for  $\text{TiH}_{1.90}$  and  $\text{TiH}_{1.81}$ . The break in curvature near 300 °K for these three samples are associated with the tetragonal deformation which occurs around this temperature for high-concentration hydrides. The fact that it is  $(T_{1e}T)^{-1/2}$  that brings out the strong break at the transition temperature gives further confirmation that  $(T_{1e}T)^{-1/2}$  is the parameter that is

representative of the electronic structure and proportional to the density of states at the Fermi level. The temperature dependence of the susceptibility,<sup>24</sup> Hall coefficient,<sup>30</sup> and resistivity<sup>30</sup> all show a similar break at the critical temperature.

#### B. Phenomenological model of the electronic structure

Various measurements have shown<sup>4-6</sup> that increasing the hydrogen content in metal hydrides serves to fill the energy states of the conduction band. This will also be taken as the basis for our discussion. We will also make use of some ideas presented by Schreiber, Cotts, and Merriam<sup>8-10</sup> who studied the La-H system and found evidence for a decreasing density of states and an approach towards semiconducting behavior as the maximum hydrogen concentration is approached. They also noted that the ratio of the maximum number of hydrogen atoms absorbed to metal atoms is three for yttrium and lanthanum which have a single outer  $d$  electron; two for titanium, zirconium, and hafnium having two outer electrons; and tends to one for vanadium, niobium, and tantalum which have three outer electrons. Thus a hydrogen atom seems to compensate for each  $d$  electron less than four. These and other phenomena were explained by Schreiber *et al.* on the basis of a crystal-field-type splitting of the  $d$  electrons into a doublet ( $d_\gamma$ ) and triplet ( $d_\epsilon$ ) expected from the fcc structure, with  $d_\gamma$  type orbitals having lower energies than those of  $d_\epsilon$ . Each hydrogen atom is assumed to donate its electron to the  $d$  band. The maximum hydrogen concentration is then obtained when the  $d_\gamma$  subband is filled with its four electrons, accounting for the decreasing density of states and semiconducting gap when the maximum hydrogen concentration is approached.

However, the  $\chi$  and  $(T_{1e}T)^{-1/2}$  concentration dependences for Ti-H do not indicate an approach to zero density of states for  $x=2$ , and the hydride is metallic rather than approaching semiconducting behavior. Furthermore, band calculations for fcc  $d$ -band metals<sup>31-34</sup> do not show complete band splitting. Thus rather than assuming a complete physical splitting of the  $d$  band, we ascribe different bonding characteristics to titanium  $d_\gamma$  orbitals and  $d_\epsilon$  orbitals with the hydrogen atoms. This can be expected since the latter are located at the vertices of a cube having a titanium atom at its center and the  $d_\gamma$  orbitals have their lobes pointing in the direction of the cube faces while the  $d_\epsilon$  lobes are directed towards the cube edges. In addition, Mott<sup>35</sup> has emphasized that the first two  $d$  subbands, which are of the bonding type (and thus designated by  $d_\gamma$  here), can

be distinguished from the other three antibonding subbands ( $d_a$ ) by the fact that  $d_a$  have nodes between the atoms while the  $d_b$  bonding states have their wave functions spread out.<sup>36</sup> Also, a number of studies have shown<sup>31,32,37,38</sup> that some  $d_\gamma - d_\epsilon$  splitting does take place for fcc transition metals and compounds with  $d_\gamma$  orbitals occupying the lower energies while the high-energy portion of the  $d$  band is  $d_\epsilon$  type. Thus  $d_b$  should be primarily  $d_\gamma$  type and  $d_a$  mainly  $d_\epsilon$  type.

Taking these arguments into consideration, we make the phenomenological assumption that *every  $d_b$  orbital for which a corresponding hydrogen atom exists with which it can interact, becomes occupied by an electron.* Thus each hydrogen atom contributes an electron to the  $d_b$  subband. Since  $d_b$  and  $d_a$  intersect,  $d_a$  states must be filled at the same time. A mechanism for supplying the extra electrons could be a movement of the  $d$  band to lower energies with respect to the  $s$  band, dumping electrons from the  $s$  band into the  $d$  band. Analyses of band calculation techniques<sup>39</sup> have shown that very slight changes in the potential function can have very large effects on the relative positions of the  $s$  and  $d$  bands. This was also seen directly by the introduction of hydrogen potentials in Switendick's band calculations of yttrium hydride<sup>13</sup> (although Switendick's extrapolation to the case of Ti-H is at variance with the present model). Similar arguments were proposed by Dugdale and Guenault<sup>40</sup> for the case of Ag in Pd and by Eastman *et al.*<sup>41</sup> for H in Pd.

The titanium atom has an outer structure of  $3d^24s^2$ . Hence in its atomic state the  $4s$  level is fully occupied. If it retains this property in the solid, then the  $4s$  band will be mostly below the Fermi level. We thus have a wide  $4s$  band filled with its quota of two electrons and a narrow  $d$  band containing two electrons. As hydrogen is added any one of a number of things can occur to fulfill the conditions of our postulates. For example, the hydrogen states may form above the Fermi level filling the conduction band with the electrons (similar to the case of TiC,<sup>31</sup> where the carbon  $p$  states form above the Fermi level and donate their electrons to the Ti  $d$  band), or hydrogen-titanium hybridized bonding states can form with the  $d_b$  orbitals, modifying already existing states without adding new ones so that one electron is contributed for each hydrogen atom.<sup>41</sup> We assume that the interaction will occur only with  $d_b$ -type orbitals. When the  $d_a$  overlap region is encountered and a  $d_b$  orbital is filled for every hydrogen atom, the material finds that it must also fill  $d_a$  states. Since the contribution of the hydrogen electrons to the  $d_b$  band lowers the total energy, the structure must adjust itself slightly

in such a way as to cause the  $d$  band to shift down with respect to the  $s$  band and thus fill the necessary  $d_a$  states. Hence we are left with the explanation that the maximum  $x$  occurs when all the  $d_b$  states are filled even when we have overlapping subbands. In a figurative way, we can consider it *as if* the hydrogen supplies the  $d_b$  states while the  $4s$  electrons supply the  $d_a$  states. An important aspect of this discussion is that according to this description, if one wants to determine the Fermi level in the overlapping  $d_b - d_a$  region, one must count only  $d_b$  states for each hydrogen atom.

It is instructive to see in a qualitative way how this model fits in with actual band structure calculations. Watson, Misetich, and Hodges<sup>42</sup> have published the density-of-state diagram showing the individual bands for the fcc metal copper which also has an outer shell configuration consisting of  $3d$  and  $4s$  electrons. This diagram was taken by the authors to generally characterize the transition as well as noble metals. As pointed out by Friedel,<sup>43</sup> transition metals with the same crystal-line structure should have similar  $d$ -band structures, little effected by the place in the Periodic Table. Thus, the general features of the  $d$ -band configuration should be retained in our semirigid-band description, with the most important difference lying the relative positions of the  $d$  and  $s$  bands, as argued previously. In fact, there is a tendency for the  $d$  band to lie higher with respect to the  $s$  band as one moves to the lighter elements in a transition-metal row.<sup>42</sup> We will assume this to hold for our case so that the major difference between our description and the diagram given by Watson *et al.* is that we will assume the  $s$  band to lie primarily below the  $d$  band. This is indeed the case for the atomic configuration which is  $3d^24s^2$  for titanium and  $3d^{10}4s$  for copper.

In Fig. 5 we reproduce the portion of the density-of-state diagram of Watson *et al.* which is pertinent to our discussion, namely the region where the first two subbands intersect the higher subbands. The horizontal scale has been expanded for clarity and the total density is shown by the solid line. Although the orbital symmetry of the states in the subbands was not given, Watson *et al.* state that the fifth subband is almost purely  $t_{2g} - d$  character. Hence it is reasonable to assume that in the cubic splitting of the  $d$  bands,  $d_\gamma$  lies below  $d_\epsilon$  in accord with our previous discussion. We associate the first two bands of Watson *et al.*'s density-of-state diagram with  $d_b$  and the 3rd, 4th, and 5th bands with  $d_a$ . Figure 5 shows the position of the Fermi level as a function of  $x$  using our previous prescription that the Fermi level is determined by counting states as if each hydrogen atom contributes one electron to the  $d_b$  subband only. We

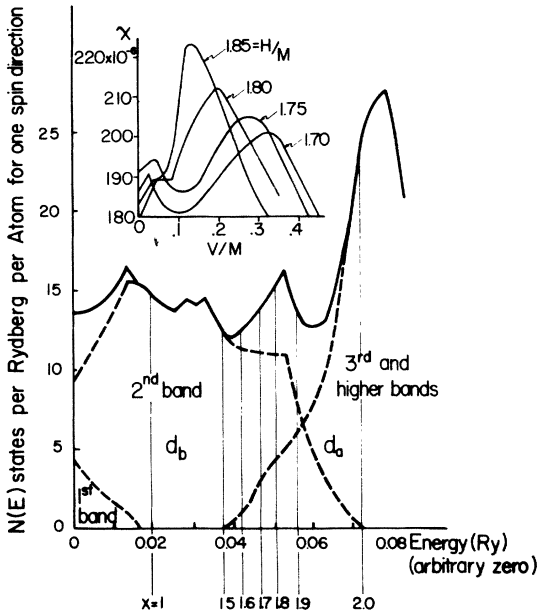


FIG. 5. Portion of the density-of-state diagram of Watson *et al.* (Ref. 42) representative of fcc transition and noble metals in a rigid-band model. The broken lines represent the individual bands while the total density is shown by the solid line.  $d_b$  denotes the first two, while  $d_a$  denotes the 3rd and higher  $d$  bands. The vertical lines are the Fermi levels for various hydrogen concentrations determined by the method described in the text. The insert shows the magnetic susceptibility  $\chi$  as a function of vanadium content for various hydrogen concentrations in Ti-V-H [ $\chi$  data of Nagel *et al.* (Ref. 14)].

see that there is a qualitative similarity between the density of states of Fig. 5 from  $x=1.5$  to  $x=2$  to the shape of the  $(T_{1e}T)^{-1/2}$  and susceptibility curves of Figs. 3(a) and 3(b). At  $x=1.5$  where the onset of the  $\gamma$  phase takes place,  $(T_{1e}T)^{-1/2}$  begins to drop just as does the density of states. Further decrease in the density of states is interrupted by the overlap with the  $d_a$  subband so that at  $x=1.6$  both the density of states and  $(T_{1e}T)^{-1/2}$  begin to rise in the same manner, giving the observed bump in the region of overlap of the two subbands. The continued rise is terminated by a Van Hove type singularity resulting in a sharp drop in the vicinity of  $x=1.8$  for both  $N(E)$  and the  $(T_{1e}T)^{-1/2}$  and  $\chi$  curves. At hydrogen concentrations approaching the maximum  $x=2$ , the behavior is influenced by the steep rise in  $d_a$ . Further confirmation that Fig. 5 represents the state of affairs is obtained from the susceptibility measurements of Nagel *et al.*<sup>14</sup> They were able to increase the amount of electrons in the band beyond the value indicated by  $x=2$  in Fig. 5 by alloying with vanadium. As the vanadium content is increased, the large hump in the density of states is observed.

For smaller hydrogen concentrations, more vanadium is necessary to get across this hump, as is shown in the insert to Fig. 5.

An interesting observation is that the  $\gamma$  phase is flanked by the end of the  $d_b$  subband at the high-hydrogen-concentration limit and by the beginning of the  $d_a$  subband at the low-concentration limit (Fig. 5). The coincidence of the high-concentration limit with the termination of the  $d_b$  subband simply follows from the fundamental theory we have hypothesized for the hydride. The fact that the low-concentration limit of the  $\gamma$  phase ( $x=1.5$ ) occurs when the Fermi level is located at the edge of the  $d_a$  band may have a physical significance. We hypothesized that the affinity of the  $d_b$  orbitals for hydrogen electrons is such that every  $d_b$  orbital for which a corresponding hydrogen atom exists, becomes occupied by an electron. Up to the point where  $d_a$  starts there is no problem in satisfying the need of the  $d_b$  orbitals. Once however  $d_a$  overlap is reached, electrons must be transferred to lower-lying "parasitic"  $d_a$  states for energy reasons, involving a relative motion of  $d$  and  $s$  bands. It is therefore plausible that when hydrogen enters the metal at an average concentration of less than  $x=1.5$ , it tries to fill all the  $d_b$  states up to where  $d_a$  starts, giving a minimum hydrogen concentration of  $x=1.5$ .

Ti, Zr, and Hf all lie consecutively below each other in the IVb column of the Periodic Table and all their hydrides have similar phase diagrams. If we assume that splitting of the  $d$  band is increased when going from the  $3d$  to  $4d$  to  $5d$  elements and if we assume that the low-hydrogen-concentration limit of the  $\gamma$  phase coincides with the commencement of the  $d_a$  subband, then we should get a continuously increasing low-hydrogen-concentration limit in going from Ti-H to Hf-H (see sketch in Fig. 6). This is actually the case as is seen from Table I. We will see later that this argument also serves to explain the different tetragonal transition behavior of Ti-H, Zr-H, and Hf-H. An increase of the band splitting in going from Ti-H to Zr-H is also supported by the specific-heat measurements of Ducastelle *et al.*<sup>45</sup> They found that while the density of states increases for Ti-H as the high-concentration limit is approached, it decreases for Zr-H. Also the density of states for ZrH<sub>1.96</sub> is half that of the titanium hydride having the same hydrogen concentration. These facts are consistent with an increase in splitting between  $d_a$  and  $d_b$  in going from Ti-H to Zr-H.

Let us now turn to the  $x=1.8$  region. It is well known that a tetragonal deformation occurs for high hydrogen concentrations above this value. The sudden drop of  $(T_{1e}T)^{-1/2}$  and  $\chi$  and the onset of the low-temperature tetragonal distortion, all

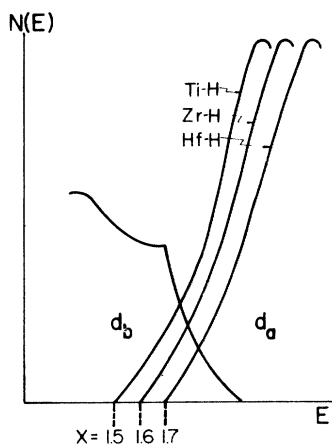


FIG. 6. Sketch of proposed behavior of  $d_a-d_b$  splitting in going down the IVb column of the Periodic Table, explaining the low-hydrogen-concentration limit, tetragonal transition, and electronic specific-heat behavior in going from Ti-H to Zr-H to Hf-H.

occur in the region of  $x = 1.8$ , the concentration at which the Fermi level lies near a Van Hove singularity of our model. It is thus natural to assume that the cause of the distortion is associated with the sharp drop in density of states at this singularity.

The electrical transport properties are also consistent with this description. Bickel and Berlincourt<sup>46</sup> measured the hydrogen-concentration dependence of the transport properties of Zr-H which is very similar to Ti-H. They found that the Hall coefficient changes from positive to negative with increasing hydrogen concentration. They interpret their data using an overlapping electron and hole band model where the hole band gets filled with increasing  $x$ . If we associate the practically full  $d_b$  subband with the hole band and the  $d_a$  band (or possibly an overlapping 4s band) with the electron band, then the filling up of  $d_b$  as  $x$  increases together with an increasing occupation of the practically empty  $d_a$  subband would explain why the Hall coefficient changes from positive to negative with increasing  $x$ . Bickel and Berlincourt also found puzzling a bump near  $x = 1.6$  which they obtained in all their transport measurements. This could be related to the similar bump in  $T_1$  we find at this concentration and which we have associated with the overlapping region of the two subbands.

We have thus presented a model which (i) gives a possible interpretation of the general behavior of  $(T_1 T)^{-1/2}$  and  $\chi$  as a function of  $x$ ; (ii) is consistent with calculations<sup>13</sup> which show that the behavior is not strictly rigid-band-like; (iii) is consistent with experimental results<sup>5-7</sup> showing that hydrides behave as if we had a rigid band with electrons

from the hydrogen being donated to the  $d$  band; (iv) retains the association of a maximum hydrogen concentration with a complete filling of the  $d_b$  band even though there may be  $d_a$  overlap; (v) suggests an explanation for the minimum and maximum hydrogen concentration field for the  $\gamma$  phase; (vi) gives a possible reason for the tetragonal-cubic transition in Ti-H above a certain concentration; and (vii) is consistent with the transport properties.

### C. Hyperfine interactions according to proposed model

We are now in a position to discuss in more detail the interactions responsible for the magnetic susceptibility, the relaxation time, and the Knight shift shown in Fig. 3. The fact that the same interaction must explain the behavior of all three parameters limits the different possibilities and leads us to certain conclusions which differ from previously proposed explanations.<sup>22,47</sup>

Let us first consider the susceptibility. Frisch and Forman<sup>26</sup> found the titanium Knight shift in titanium hydride to be positive and independent of hydrogen concentration and temperature. An analysis<sup>48</sup> of their data and that of the Knight shift<sup>49</sup> and susceptibility<sup>50</sup> of pure titanium shows that the primary interactions are of orbital origin, and that for titanium hydride the orbital and  $s$ -electron contributions to the susceptibility are largely independent of the hydrogen concentration and given by  $\chi_0 \approx 100 \times 10^{-6}$  emu/hole and  $\chi_s \approx 20 \times 10^{-6}$  emu/mole. Subtracting  $120 \times 10^{-6}$  emu/mole from the total susceptibility shown in Fig. 3(b) for  $T = 290$  and  $80^\circ \text{K}$ , and using Eq. (1) to obtain the density of states at the Fermi level, results in curves Fig. 7(a) and 7(b). We compare their shapes to that of Fig. 7(c), which is the density of states at the Fermi level as a function of hydrogen concentration obtained from the density-of-state diagram of Fig. 5 using the previously described method of counting states when the hydrogen concentration is varied. We note a close similarity of Figs. 7(a) and 7(b) to that of Fig. 7(c).

We now consider the hyperfine interaction  $H_{hf}$  responsible for the hydrogen Knight shift and spin-lattice relaxation. Direct  $s$  conduction-electron

TABLE I. Low-hydrogen-concentration limit of IVb transition-metal hydrides.

Hydride	$x$ at $\gamma$ to $\alpha + \gamma$ interface	Reference
Ti-H	1.5	Refs. 17 and 23
Zr-H	1.6	p. 246 of Ref. (44)
Hf-H	1.7	p. 322 of Ref. (44)



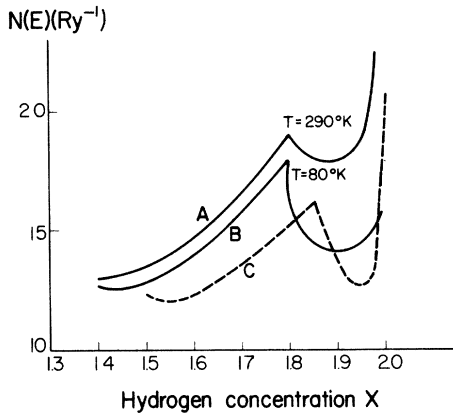


FIG. 7. Density of states at Fermi level as a function of hydrogen concentration, derived from the susceptibility measurements of Trzebiatowsky *et al.* [(a) and (b)—see Fig. 3(b)], compared to the density-of-states diagram of Watson *et al.* (c), using theory discussed in text.

interaction must be ruled out since firstly the  $s$  component of the density of states should vary only slightly with the position of the Fermi level, and second, would give a positive Knight shift rather than the observed negative value.<sup>22</sup> Comparing the hydrogen Knight shift with  $(T_{1e}T)^{-1/2}$  in Fig. 3, we note that whereas the former is practically constant between  $x = 1.6$  and  $x = 1.85$ , the latter increases sharply in this region. Even if we ascribe this constancy of the Knight shift to some fortuitous cancellation of positive and negative components, it is extremely unlikely that the cusplike shape would remain undetected if one of the components were proportional to the same interaction as  $(T_{1e}T)^{-1/2}$  is. Equations (2) and (3) indicate, that if the hyperfine interaction were due to the core polarization by hybrid titanium  $d$  states<sup>47</sup> (explaining the negative shift) then both the shift and  $(T_{1e}T)^{-1/2}$  should show similar behavior, contrary to experiment. The only interaction for which  $(T_{1e}T)^{-1/2}$  and  $K$  are expected to differ is the orbital one since for this case only does  $(T_{1e}T)^{-1/2}$  depend on the density of state at the Fermi level while  $K$  is influenced by the status of the entire band. We thus conclude that the primary interaction responsible for the spin-lattice relaxation and Knight shift is orbital so that by and large we may write

$$(T_{1e}T)^{-1/2} \approx (4\pi\gamma_n^2 \hbar k_B)^{1/2} (H_{\text{hf}}^{(0)})(p)^{1/2} N_d(E_F). \quad (4)$$

All this is consistent with the analysis which contends that it is the orbital interaction that is probably responsible for the titanium Knight shift and a major contributor to the magnetic susceptibility of the hydride.

The fact that the Fermi level is swept through the region where  $d_b$  and  $d_a$  overlap should affect the concentration dependence of  $(T_{1e}T)^{-1/2}$  somewhat through the reduction factor  $p$ , accounting for some of the differences in the shape of  $\chi$  and  $(T_{1e}T)^{-1/2}$ . A comparison<sup>48</sup> of  $(T_{1e}T)^{-1/2}$  with the Knight shift through an approximate Korringa relation seems to support an orbital interaction relaxation mechanism. A rough analysis<sup>48</sup> using our relaxation data and an orbital reduction factor for cubic symmetry gives a fairly constant value for the orbital hyperfine field at the proton of  $H_{\text{hf}}^{(0)} = 9.7, 7.5, 8.7, 8.7, \text{ and } 8.2 \text{ kG}$  for  $x = 1.6, 1.7, 1.8, 1.9, 2.0$ , respectively. This is approximately  $\frac{1}{20}$  of the orbital hyperfine field for titanium which is about 160 kG.<sup>49</sup>

Using these values of the hyperfine field and our previous estimate  $\chi_0 \approx 100 \times 10^{-6} \text{ emu/mole}$  we can obtain the calculated Knight shift from Eq. (2) where only the orbital term  $K_0$  contributes and the usual approximation  $H_{\text{hf}}^{(0)} \approx H_{\text{hf}}^{(0)'}$  is made. These calculated shifts are plotted in Fig. 3(c) together with Stalinski's measured results and show agreement over the entire concentration range except near  $x = 2$ . The discrepancy at this point cannot be attributed to an increase in  $\chi_0$  since, among other arguments,<sup>48</sup> the titanium Knight shift in the hydride is independent of the hydrogen concentration.<sup>26</sup> One possible explanation would be that the assumption  $H_{\text{hf}}^{(0)} \approx H_{\text{hf}}^{(0)'}$  breaks down, i.e., there may be an increase in  $H_{\text{hf}}^{(0)'}$  near  $x = 2$  without a corresponding increase in  $H_{\text{hf}}^{(0)}$ .

A few words about the hyperfine interaction with the protons is appropriate at this point. Very often the orbital hyperfine field at the nucleus is approximated by its value for the free atom.<sup>28</sup> Since this must always be positive, one generally considers the orbital contribution to the Knight shift to be positive. The proton Knight shift in Ti-H is however negative<sup>18</sup> and we are attributing this to an orbital interaction. This can be understood by noting that in our case we are considering a transfer of the interaction to a neighboring atom, i.e., the influence of the orbital electrons of the host atom on a nearby nucleus. In analogy with an analysis of the orbital interaction for nonmetals,<sup>51</sup> the resonance shift tends to decrease and may become negative as the distance from the center of the electron distribution increases. Intuitively, one can surmise that an unquenching of the angular momentum giving a net circular current in say a clockwise direction, can result in counterclockwise sense for an external nucleus. This could then result in a negative Knight shift. There are a number of cases where when a metal having a positive Knight shift is alloyed with a host metal whose hyperfine interaction is primarily orbital, the Knight

shift of the substitutional metal is reduced to a small fraction of its value and may even become negative. This can be seen for example for the case of Al and Sn in  $\text{Nb}_3\text{Al}$  and  $\text{Nb}_3\text{Sn}$ .<sup>52</sup> Thus while the approximation  $H_{\text{hf}}^{(0)} \approx H_{\text{hf}}^{(0)'} \approx H_{\text{hf(atom)}}^{(0)}$  may be valid for the nuclei of the host metal, it is not expected to hold for the substitutional or interstitial nuclei.

#### D. Thermal effects and the tetragonal deformation

Many of the properties we have been discussing are temperature dependent. We must see how this dependence and our  $(T_{1e}T)^{-1/2}$  results (Fig. 4) can be understood in the general context of our model.

Both Gesi *et al.*<sup>53</sup> and Ducastelle *et al.*<sup>45</sup> have attempted to explain thermal effects in Ti-H in terms of the electronic structure. We associate the tetragonal deformation with the Van Hove singularity occurring near  $x=1.8$ . By directing our attention to the  $(T_{1e}T)^{-1/2}$  and  $\chi$  curves of Figs. 3(a) and 3(b), we see that raising the temperature tends to fill up the trough in the region  $1.8 < x < 2.0$ . This would occur if part of the  $d_a$  band moves to the left as the crystal structure becomes less tetragonal. This leftward movement would cause a larger rate of increase in the density of states at high concentration than at low concentration which seems indeed to be the case, as reflected in the temperature-dependence behavior of  $\chi$ ,<sup>24</sup> and  $(T_{1e}T)^{-1/2}$  (Fig. 4) in the tetragonal phase. The motion of  $d_a$  does not have to be looked upon as being rigid as will become clearer later when discussing possible mechanisms for the movement. The shift in  $d_a$  is a direct result of the tetragonal deformation. As the trough fills up with increasing temperature, the sudden drop in the density of states near the Van Hove singularity becomes less severe and consequently, so does the tetragonal deformation. When  $d_a$  is far enough to the left, the singularity becomes so weak that the tetragonal deformation disappears completely (at about 310 °K). When the concentration is low so as to place the Fermi level far enough to the left of the Van Hove singularity, there is no tetragonal deformation.

This analysis also suggests why high-concentration zirconium and hafnium hydrides remain tetragonally deformed even at high temperature.<sup>20,21</sup> Although the  $c/a$  ratio increases towards unity with increasing temperature, the cubic phase is never reached. According to our previous hypothesis (see discussion of Fig. 6), the  $d$ -band splitting of Zr-H and Hf-H is larger than that of Ti-H. Thus the leftward movement of  $d_a$  with increasing temperature is unable to wipe out the Van Hove singularity and the structure remains tetragonal.

There are two possible mechanisms that can be responsible for the distortion of  $d_a$  with the tetragonality of the crystal structure. According to our thesis in which the central theme is the crystal-field-type splitting of the  $d$  band into a doublet ( $d_b$ ) and triplet ( $d_a$ ) when the titanium atoms find themselves in a cubic environment, we must perforce also take into account that the triplet should then split further into a singlet and a doublet under a tetragonal deformation. The greater the crystallographic deformation the larger the splitting. Thus a tetragonal deformation should be accompanied by a deformation of the  $d_a$  subband, filling up the trough. This argument has some features in common with the discussion of Ducastelle *et al.*<sup>45</sup> for the case of Ti-H, Zr-H, Hf-H, and Labbé and Friedel<sup>54</sup> in their explanation of the tetragonal deformation of  $\text{V}_3\text{Si}$  and  $\text{Nb}_3\text{Sn}$ .

Another effect which must be included when considering the tetragonal deformation is the accompanying distortion of the Brillouin zone. The hexagonal portion of the zone surface for the fcc structure, which is the face that lies closest to the center of the zone, moves outward under tetragonal distortion. Thus one would expect the filling of a new band to occur at higher energies, resulting in a movement of  $d_a$  towards the right as the temperature decreases and the tetragonality increases. An exact analysis is beyond present capabilities, but be as it may, the temperature-dependence curves of  $(T_{1e}T)^{-1/2}$  and  $\chi$  for high hydrogen concentrations show that the density of states for a given  $x$  drops with increasing tetragonality. [Compare  $(T_{1e}T)^{-1/2}$  with  $c/a$  as function of  $T$  for  $x=1.99$  in Fig. 4.]

Let us now consider in more detail the temperature-dependence curves of  $(T_{1e}T)^{-1/2}$  (Fig. 4) and  $\chi$ ,<sup>24</sup> and focus our attention first on the high-concentration sample  $\text{TiH}_{1.99}$ . Both  $(T_{1e}T)^{-1/2}$  and  $\chi$  increase with temperature in the tetragonal phase, but in the cubic phase  $(T_{1e}T)^{-1/2}$  is constant while  $\chi$  decreases with increasing temperature. There are two effects acting simultaneously. The primary one is the tendency of  $(T_{1e}T)^{-1/2}$  and  $\chi$  to increase with temperature due to the previously discussed lattice distortion. The secondary one concerns the shift in Fermi level and the widening of the Fermi distribution about this level with increasing temperature which for the susceptibility takes the form<sup>2</sup>

$$\chi(T) = 2\mu_B^2 N(E_f) \left\{ 1 + \frac{1}{6} \pi^2 k_B^2 T^2 \left[ \frac{1}{N(E)} \frac{d^2 N(E)}{dE^2} - \left( \frac{1}{N(E)} \frac{dN}{dE} \right)^2 \right]_{E=E_f} \right\}, \quad (5)$$

and for the relaxation time is given by<sup>55</sup>

$$\frac{1}{T_{1e}(T)T} = \frac{1}{T_{1e}(0)T} \left[ 1 + \frac{1}{3}\pi^2 k_B^2 T^2 \left( \frac{1}{N(E)} \frac{d^2 N}{dE^2} \right)_{E=E_f} \right]. \quad (6)$$

The second derivative term should be weak enough to be neglected in both Eqs. (5) and (6). Thus when the temperature increases from 100 °K, the negative term in Eq. (5) is overshadowed by the effect of the increase in the density of states resulting from a lessening of the tetragonal deformation, and both  $(T_{1e}T)^{-1/2}$  and  $\chi$  rise rapidly. When the transformation temperature is reached and distortion of the  $d$ -band structure ceases, only the negative term in Eq. (5) influences the susceptibility resulting in a relatively small drop with temperature while  $(T_{1e}T)^{-1/2}$  becomes constant since no comparable negative term exists in Eq. (6). A similar argument holds for the lower hydrogen concentration samples when  $x > 1.8$  but to a lesser degree since the Fermi level is too far away to sense the full impact of the distortion of  $d_a$  and the derivative of the density of states at the Fermi level is smaller. The samples having hydrogen concentrations less than  $x = 1.8$  do not undergo a tetragonal distortion and thus display no break in the  $(T_{1e}T)^{-1/2}$  curves. Presumably the small gradual rise in  $(T_{1e}T)^{-1/2}$  reflects changes in the crystallographic parameters, such as a general increase in the density of states under lattice ex-

pansion.

The problem concerning the tetragonal deformation in Ti-H has been widely discussed<sup>20,23,29,56</sup> and there is a considerable disagreement as to its origin, the hydrogen concentration above which it occurs and the transition temperature.

As to its origin, Bale and Peterson<sup>56</sup> claim that the cause for the transition has not been established, and dispute the contention of Azarkh and Gavrilov<sup>23</sup> that an order-disorder transformation of the hydrogen positions is involved. The theory presented here attributes the transition to a Van Hove singularity in the density of states.

There is also wide disagreement as to the concentration range and temperature for the transition. While Azarkh *et al.*<sup>23</sup> found the tetragonal range to begin at about TiH<sub>1.75</sub>, Irving *et al.*<sup>29</sup> observed it to begin at TiH<sub>1.9</sub>. If one assumes that the discontinuities in the temperature dependence of the physical parameters are due to the phase transition, the observations of numerous investigators can be compared. Figure 8 shows the results outlining the tetragonal phase region, with the solid line presumptuously drawn through the points obtained in this investigation.

Although some of the discrepancies may be attributed to uncertainties in hydrogen concentration, and Irving *et al.* believe them to be due to impurity content, it is obvious from the work of Azarkh and Gavrilov that there are more fundamental processes, probably connected with internal stress, that must be taken into account. The latter investigators found that some samples did not give tetragonal distortions unless they were subjected to heating at about 500 °C for more than 5 h and that the tendency for the cubic phase to be retained increases as the limiting concentration  $x = 2$  is approached. Irving and Beevers also found no tetragonal deformation for their highest concentration sample of TiH<sub>1.99</sub>. Thus the contribution of internal stresses to the free energy is probably not negligible and must be taken into account in addition to the main electronic energy band considerations previously discussed.

A theory concerning the inconsistencies presents itself if we also take into consideration a further result of the x-ray studies<sup>20,56</sup> that a characteristic broadening of the reflection occurs just below the critical temperature except for those of the form  $\{h\bar{h}h\}$ . Since the cubic axes of the fcc structure are equivalent, the  $c$  axis of the tetragonal structure may take any of three directions, smearing out the tetragonality properties of the material. Thus the doublet due to the tetragonal splitting of the (200) and (002) reflections for example may spread out due to the uncertainty in the choice of the  $c$  axis in the Bragg formula in

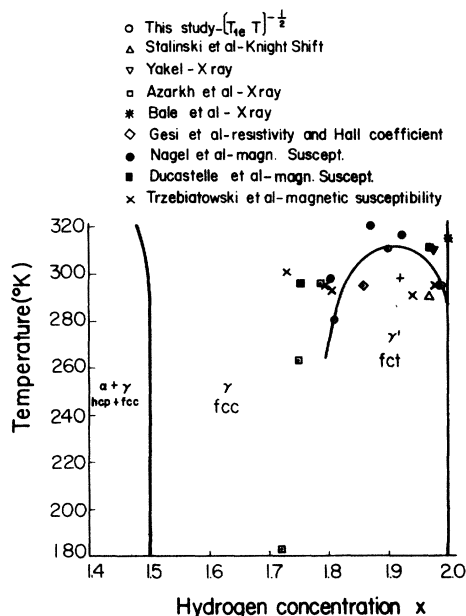


FIG. 8. Tetragonal-cubic transition region derived from our measurements and those of Refs. 14, 20, 22, 23, 24, 30, 45, and 56.

$$\sin^2\theta = \frac{1}{4}\lambda^2 \left[ \frac{h^2 + k^2}{a^2} + \frac{l^2}{c^2} \right].$$

When  $h = k = l$ , however, the choice of the  $c$  axis is irrelevant and we may expect sharp reflections. Thus near the transition temperature the material may behave on the average as cubic if there are equal amounts of material with  $c$  axes in the [100], [010], and [001] directions without long-range order. This behavior should depend on internal stresses so that a spread in results of different investigations may occur, and presumably also a retention of cubic behavior in the normally tetragonal region. The order causing stresses which may be expected at vacancies in the nonstoichiometric hydride are absent for the stoichiometric composition suggesting why x-ray measurements indicate that it is easier to retain the artificial average "cubic" phase in the limit of  $\text{TiH}_2$ . This kind of phenomenon has also been ascribed<sup>57,58</sup> to the martensitic tetragonal deformation in  $\text{V}_3\text{Si}$  and  $\text{Nb}_3\text{Sn}$ . (The Ti-H tetragonal deformation is also martensitic.<sup>29</sup>)

Turning now to the temperature dependence of the transport parameters, Gesi *et al.*<sup>30</sup> found that the rate of increase of resistivity and Hall coefficient with temperature decreases discontinuously at the transformation from tetragonal to cubic phase. Following Bickel *et al.*<sup>46</sup> who interpret their data in terms of an overlapping electron and hole band, we attribute the increase in resistivity with temperature to the usual phonon scattering into empty states of the  $d$  band.<sup>2</sup> Since this is proportional to the density of states at the Fermi level, the increase of resistivity with temperature is faster below the critical temperature than above it because, as seen from Fig. 4, the density of states also rises with temperature in the tetragonal phase and stops rising abruptly in the cubic phase. Assuming that the increased scattering with increasing density of states lowers the electron mobility with respect to the hole mobility would also explain the more rapid increase of the Hall coefficient below the critical temperature.

#### E. General remarks on bonding in the hydride

All the properties show that the hydride is obviously metallic. Inelastic neutron scattering<sup>59</sup> and hydrogen diffusion<sup>60</sup> measurements indicate however that the hydrogen is held in its equilibrium position in a narrow potential well that is independent of the hydrogen concentration which could be indicative of a covalent bond. Furthermore, the Knight shift and spin-lattice relaxation rates of the hydrogen are much too small if the hydrogen bond were simply metallic. Thus we must be able to look at the hydride from two sep-

arate points of view: one is the metallic nature of the Ti bonds which allows us to make calculations based on the density of states as if the hydride were a metal, and the other is the local covalent bond formed between the titanium and hydrogen atoms. Such a dual outlook is not unique to the hydride but is also a general property of the refractory hard metals that are formed between certain transition metals (such as titanium) and nonmetallic elements (such as carbon). The bonding scheme for these metals has been discussed by Lye *et al.*<sup>31,61</sup> and Costa *et al.*<sup>62</sup> using experimentally adjusted band calculations. Their results exhibit many properties that are similar to our model. They claim<sup>62</sup> that in order to understand the nonstoichiometric nature of the compounds, it is useful to consider the transition metal as a possible acceptor of electrons where the interstitial atom transfers electrons to the  $d$  band of the metal, and that this type of model permits a metal-metal type binding through the  $d$  orbitals in addition to the metal-nonmetal type bonding. It is also shown that the introduction of carbon potentials markedly influence the  $d$ - $d$  interactions between the metal atoms, and as a result bonding states of the  $d$  states are depressed in TiC to energies lower than they would have in (hypothetical) fcc titanium.<sup>61</sup> We have similarly argued that with the addition of more hydrogen potentials, the  $d$  band is lowered with respect to the  $s$  band, filling up the state of the former. We have hypothesized that the  $d_b$  band gets filled to a maximum of four electrons, the extra electrons to fill this and the overlapping  $d_a$  region coming from the hydrogen and  $4s$  band. This can be compared to the case of Ti-C,<sup>61</sup> where the calculations show that the electronic configuration is approximately  $(2s)^2(2p)^{3/4}$  for carbon and  $(3d)^4(4s)^{3/4}(4p)^{1/2}$  for titanium compared to the isolated atom configuration of  $(2s)^2(2p)^2$  and  $(3d)^2(4s)^2$ , respectively. That is, the electrons that fill the  $4d$  band to a total of four electrons come from the carbon and  $4s$  band. The density-of-state diagram of Lye *et al.*<sup>31,61</sup> show two overlapping  $d_\gamma$  and  $d_\epsilon$  subbands, with the latter occupying mainly the high-energy states.

Band calculations of some rare-earth hydrides were performed by Switendick<sup>13</sup> and it is questionable whether his conclusions can be incorporated into the picture described here. A basic uncertainty of these calculations is the assumption that the removal of hydrogen from random sites can be described by the turning on and off of the hydrogen potential in the entire lattice.

The low-hydrogen-concentration limit of the  $\gamma$  phase again emphasizes the dual nature of the hydride. At low temperature this limit is given by

$x = 1.5$ . If however the temperature is raised,  $x$  can be lowered, presumably due to the contribution of the entropy term in the free energy. The phase diagram of Ref. 17 shows that  $x$  can attain a value as low as 1.0 at 250 °C. There are two independent measurements<sup>17</sup> which show however that in this higher-temperature region the hydrogen is not distributed randomly, but clusters to retain a local concentration of about  $x = 1.5$ . The first is the hydrogen diffusional jump frequency which is proportional to the number of vacancies up to  $x = 1.5$ . Lowering the concentration below this limit causes the proportionality curve to level off as if the local hydrogen distribution is still about  $x = 1.5$ . The second is  $T_{1d}^{\text{min}}$  which is the minimum of the temperature-dependent spin-lattice relaxation time due to diffusion. This value is simply a function of the distance between hydrogen atoms. While the measurements follow a curve consistent with a random distribution of the hydrogen among the tetrahedral sites down to  $x = 1.5$ , when the concentration is lowered below this value (at high temperature),  $T_{1d}^{\text{min}}$  levels off, indicating clustering giving a local concentration of about  $x = 1.5$ . Thus when viewing the general phase diagram and crystallographic structure, it is the electronic band structure and entropy term that is of importance. In the local picture however, we may surmise that a minimum of three hydrogen to two titanium atoms ( $x = \frac{3}{2} = 1.5$ ) are necessary to form the local covalent bond and this will be so even when the temperature is high enough for the fcc structure to be maintained below  $x = 1.5$ . The brittleness of the hydride compared to the pure metal has also been ascribed to a local Ti-H covalent behavior.

#### V. SUMMARY AND CONCLUDING REMARKS

The view taken is that the variation of the physical properties of Ti-H as the concentration  $x$  is changed can be described by a semirigid-band model derived for the fcc structure, whereby the  $d$ -electron states are filled with electrons as the hydrogen concentration  $x$  is increased. It is asserted that due to the different geometric shapes of their wave functions, the hydrogen bonding properties of the first two  $d$  subbands ( $d_b$ ) differ from that of the last three ( $d_a$ ) in that one electron will be contributed to  $d_b$  for each hydrogen atom dissolved. Since there is overlap between  $d_b$  and  $d_a$ , the extra electrons are supplied from the  $s$  band by the shift of the relative positions of the  $d$  and  $s$  bands with increasing hydrogen concentration. This method of locating the Fermi level

gives a qualitative correlation between the fcc density-of-state diagram with  $(T_{1e}T)^{-1/2}$  and susceptibility measurements as the hydrogen concentration (and vanadium concentration) is varied. The model also suggests why  $d^1, d^2, d^3$  metals tend to absorb a maximum of three, two, one hydrogen atoms per metal atom (filling up the  $d_b$  subband). The low-hydrogen-concentration limit  $x = 1.5$  is associated with the onset of the  $d_a$  band (since up to this concentration the  $d_b$  states per hydrogen atom can be filled without having to supply extra electrons to the  $d_a$  band). The low-temperature tetragonal deformation is associated with a Van Hove singularity of  $d_b$ . The temperature dependence of  $\chi$  and  $(T_{1e}T)^{-1/2}$  below the transformation temperature for various hydrogen concentrations show that  $d_a$  is distorted in such a way as to result in a net movement towards lower energy, wiping out the singularity and removing the tetragonal deformation. Assuming that  $d_b - d_a$  splitting increases as we go to heavier  $d^2$  metals (as supported by specific-heat measurements) explains why the low-limit hydrogen concentration for Zr and Hf goes up, and why the crystal structure of Zr-H and Hf-H remain tetragonal even at higher temperatures. The change of the transport properties with hydrogen concentration and temperature are also shown to be consistent with the model presented here.

Our measurements also support the contention that the major magnetic interactions derive from orbital effects and that the hyperfine interaction with the hydrogen is approximately 9 kG, more than an order of magnitude weaker than that at the titanium nuclei.

The model presented is phenomenological and speculative. Its claim to merit serious consideration is that a considerable number of physical phenomena can be explained and correlated with its use. Although great strides have been made in recent years in the calculation of band structure from first principles, the large sensitivity of the results to unknown potentials and other fine effects have not yet permitted these methods to yield unambiguous and unique electronic structures. The problem is compounded for nonstoichiometric materials which cannot yet be tackled in a straightforward manner.

#### ACKNOWLEDGMENT

I would like to thank Dr. D. Zamir, Dr. S. Alexander, and Dr. M. Weger for many helpful discussions, and K. Levin for his able technical assistance.

- \*Research sponsored in part by the Air Force Materials Laboratory, United States Air Force, under grant No. AF OSR-72-2310.
- <sup>1</sup>B. Stalinski, Ber. Bunsenges. Phys. Chem. 76, 724 (1972).
- <sup>2</sup>N. F. Mott and H. Jones, *Theory of the Properties of Metals and Alloys* (Dover, New York, 1936).
- <sup>3</sup>H. C. Jamieson and F. P. Manchester, J. Phys. E 2, 323 (1972); D. Shaltiel, J. Appl. Phys. 34, 1190 (1963).
- <sup>4</sup>I. Isenberg, Phys. Rev. 79, 736 (1950).
- <sup>5</sup>D. Zamir, Phys. Rev. 140, A271 (1965).
- <sup>6</sup>D. Rohy and R. M. Cotts, Phys. Rev. B 1, 2070 (1970).
- <sup>7</sup>D. Rohy and R. M. Cotts, Phys. Rev. B 1, 2484 (1970).
- <sup>8</sup>D. S. Schreiber and R. M. Cotts, Phys. Rev. 131, 1118 (1963).
- <sup>9</sup>D. S. Schreiber, Phys. Rev. 137, A860 (1965).
- <sup>10</sup>M. F. Merriam and D. S. Schreiber, J. Phys. Chem. Solids 24, 1375 (1963).
- <sup>11</sup>W. G. Bos and H. S. Gutowsky, Inorg. Chem. 6, 552 (1967).
- <sup>12</sup>R. Green and W. G. Bos, Phys. Rev. B 3, 64 (1971).
- <sup>13</sup>A. C. Switendick, Solid State Commun. 8, 1463 (1970).
- <sup>14</sup>H. Nagel and H. Goretzki, J. Phys. Chem. Solids 36, 431 (1975).
- <sup>15</sup>A. Abragam, *The Principles of Nuclear Magnetism* (Oxford University, London, 1961).
- <sup>16</sup>H. C. Torrey, Nuovo Cimento Suppl. 9, 95 (1958).
- <sup>17</sup>C. Korn and D. Zamir, J. Phys. Chem. Solids 31, 489 (1970).
- <sup>18</sup>A. Schmolz and F. Noack, Ber. Bunsenges. Phys. Chem. 78, 339 (1974).
- <sup>19</sup>E. F. Khodosov and N. A. Shepilov, Phys. Status Solidi B 49, K83 (1972).
- <sup>20</sup>H. L. Yakel, Jr., Acta Crystallogr. 11, 46 (1958).
- <sup>21</sup>S. S. Sidhu, L. Heaton, and D. D. Zaubers, Acta Crystallogr. 9, 607 (1956).
- <sup>22</sup>B. Stalinski, C. K. Coogan, and H. S. Gutowsky, J. Chem. Phys. 34, 1191 (1961).
- <sup>23</sup>Z. M. Azarkh and P. I. Gavrilov, Sov. Phys.-Crystallogr. 15, 231 (1970) [Kristallografiya 15, 275 (1970)].
- <sup>24</sup>W. Trzebiatowsky and B. Stalinski, Bull. Acad. Polon. Sci. 1, 131 (1953).
- <sup>25</sup>D. S. Schreiber and L. D. Graham, J. Chem. Phys. 43, 2573 (1965).
- <sup>26</sup>R. C. Frisch and R. A. Forman, J. Chem. Phys. 48, 5187 (1968).
- <sup>27</sup>See, for example, A. Narath, in *Hyperfine Interactions*, edited by A. J. Freeman and R. B. Frankel (Academic, New York, 1967).
- <sup>28</sup>See, for example, A. Narath and A. T. Fromhold, Jr., Phys. Rev. 139, A794 (1965).
- <sup>29</sup>P. E. Irving and C. J. Beevers, Met. Trans. 2, 613 (1971).
- <sup>30</sup>K. Gesi, Y. Takagi, and T. Takeuchi, J. Phys. Soc. Jpn. 18, 306 (1963).
- <sup>31</sup>R. G. Lye and E. M. Logothetis, Phys. Rev. 147, 622 (1966).
- <sup>32</sup>L. Hodges, H. Ehrenreich, and N. D. Lang, Phys. Rev. 152, 505 (1966).
- <sup>33</sup>F. M. Mueller, Phys. Rev. 153, 659 (1967).
- <sup>34</sup>J. W. D. Connolly, Phys. Rev. 159, 415 (1967).
- <sup>35</sup>N. F. Mott, Adv. Phys. 13, 325 (1964).
- <sup>36</sup>J. H. Wood, Phys. Rev. 117, 714 (1960).
- <sup>37</sup>J. Callaway, Phys. Rev. 121, 1351 (1961).
- <sup>38</sup>H. A. Mook, Phys. Rev. 148, 495 (1966).
- <sup>39</sup>J. M. Ziman, Proc. Phys. Soc. Lond. 91, 701 (1967).
- <sup>40</sup>J. S. Dugdale and A. M. Guenault, Philos. Mag. 13, 503 (1966).
- <sup>41</sup>D. E. Eastman, J. K. Cashion, and A. C. Switendick, Phys. Rev. Lett. 27, 35 (1971).
- <sup>42</sup>R. E. Watson, A. A. Missetich, and L. Hodges, J. Phys. Chem. Solids 32, 709 (1971).
- <sup>43</sup>J. Friedel, in *Physics of Metals*, edited by J. M. Ziman (Cambridge University, London, 1969), p. 344.
- <sup>44</sup>W. M. Mueller, J. P. Blackledge, G. G. Libowitz, *Metal Hydrides* (Academic, New York, 1968).
- <sup>45</sup>F. Ducastelle, R. Caudron, and P. Costa, J. Phys. (Paris) 31, 57 (1970).
- <sup>46</sup>P. W. Bickel and T. G. Berlincourt, Phys. Rev. B 2, 4807 (1970).
- <sup>47</sup>E. Ehrenfreund, M. Weger, C. Korn, and D. Zamir, J. Chem. Phys. 50, 1907 (1969).
- <sup>48</sup>C. Korn, Final Scientific Report, U.S. Air Force contract No. AF OSR 72-2310 (1975) (unpublished).
- <sup>49</sup>A. Narath, Phys. Rev. 162, 320 (1967).
- <sup>50</sup>E. W. Collings and J. C. Ho, Phys. Rev. B 2, 235 (1970).
- <sup>51</sup>Pgs. 78-79 of C. P. Slichter, *Principles of Magnetic Resonance* (Harper, New York, 1963).
- <sup>52</sup>E. Ehrenfreund, A. C. Gossard, and J. H. Wernick, Phys. Rev. B 4, 2906 (1971).
- <sup>53</sup>K. Gesi, Y. Takagi, T. Takeuchi, and S. Noguchi, in *Nuclear Metallurgy, International Symposium on Compounds of Interest in Nuclear Reactor Technology*, edited by J. T. Waber, P. Chiotti, and W. N. Miner (AIME, New York, 1964), p. 46; also quoted in Ref. 44.
- <sup>54</sup>J. Labbé, Phys. Rev. 158, 647 (1967), and references therein.
- <sup>55</sup>Y. Yafet and V. Jaccarino, Phys. Rev. 133, A1630 (1964).
- <sup>56</sup>H. D. Bale and S. B. Peterson, Solid State Commun. 11, 1143 (1972).
- <sup>57</sup>M. Weger and I. B. Goldberg, Solid State Phys. 28, 1 (1973).
- <sup>58</sup>J. Noolandi and C. M. Varma, Phys. Rev. B 11, 4743 (1975).
- <sup>59</sup>S. S. Pan and F. J. Webb, Nucl. Sci. Eng. 23, 194 (1965).
- <sup>60</sup>C. Korn and D. Zamir, J. Phys. Chem. Solids 34, 725 (1973).
- <sup>61</sup>R. G. Lye, in *Atomic and Electronic Structure of Metals*, Seminar of the American Society for Metals, American Society for Metals, Metals Park, Ohio, 1966.
- <sup>62</sup>P. Costa and R. R. Conte, in *Nuclear Metallurgy, International Symposium on Compounds of Interest in Nuclear Technology*, edited by J. T. Waber, P. Chiotti, W. N. Miner (AIME, New York, 1964), p. 3.